Educational Administration: Theory and Practice
2024, 30(4), 8874-8882
ISSN:2148-2403
https://kuey.net/

Research Article

Spatio Temporal Analysis Of Swell Waves During FANI And TITLI Cyclones Using Empirical Orthogonal Function Analysis

Susmita Biswas[1*], and Mourani Sinha[2]

[1*]Department of Cyber Science & Technology, Brainware University, Kolkata- 700125
[2]Department of Mathematics, Techno India University, West Bengal, Kolkata-700091.

***Corresponding author:** Susmita Biswas
[*]Department of Cyber Science & Technology, Brainware University, Kolkata- 700125 Email: Bi.Susmita@Gmail.Com.

Citation: Susmita Biswas Et Al. (2024), Spatio Temporal Analysis Of Swell Waves During FANI And TITLI Cyclones Using Empirical Orthogonal Function Analysis *Educational Administration: Theory And Practice*, *30*(4), 8874-8882
Doi: 10.53555/kuey.v30i4.2876

ARTICLE INFO

ABSTRACT

Intricate maritime state with the simultaneous incidence of swell, wind, and sea conditions generates high wave energies which impacts on air-sea interactions and the changing global climate. Swell waves in the ocean can often be surprisingly destructive which can cause serious damage to ships. In this study, the impact of the swell wave heights on the cyclonic wave heights occurring during reversing monsoon months was studied. TITLI was a very severe cyclonic storm (07 to 13 October 2018) and FANI was an extremely violent storm that cyclonic (26 April to 05 May 2019) over the Bay of Bengal (BOB). The impact of FANI occurring in May (pre-monsoon month) was more severe than TITLI in October (post-monsoon monsoon) over the east coast of India. Empirical orthogonal function (EOF) analysis was performed on the swell wave height data for the BOB region, to obtain the major spatial and temporal patterns prevailing. Combined wind and swell wave heights, only swell wave heights and only wind wave heights were analyzed during the cyclonic period to measure the impact of swell waves in the region.

Keywords. Empirical orthogonal function analysis; spatio temporal analysis; climate change; swell waves; tropical cyclones.

1. Introduction

Large waves evolving due to strong winds or swell waves being generated by distant storms, both can cause damaging high sea states. (Zhang and Li 2017) studied dangerous sea states triggering ship accidents. They analyzed 10 years (2001–2010) ship accident dataset from the International Maritime Organization including 3648 ship accidents. For the chosen ship accident instances, sea state characteristics from a numerical wave model, such as significant wave height, mean wave period, and mean wave direction, were examined. In the dataset, there were 1561 occurrences that still had precise geographic coordinates. Of these, 58 cases were kept for the analysis because they happened in sea conditions connected to swells. Looking at the 58 swell-related incidents, the study showed that 52% of the instances happened in relatively low sea state circumstances, meaning that the majority of the wave energy was created by the swell waves in these conditions, with significant wave height values less than 3 meters. Subsequent investigation into these incidents revealed that co-occurring wind seas and swells may provide dangerous seas and endanger maritime operations, particularly when the variations in their mean wave periods and mean wave duration satisfy specific requirements. The authors arrived at the conclusion that sailing vessels are at risk from combined sea and swell conditions, particularly when these variables contain identical wave durations and oblique wave orientations. A crossing sea is a sea condition in which two wave systems are moving at oblique angles. In the past, a few studies have indicated that the occurrence of extreme waves and serious ship accidents (Brunset *al.* 2011; Cavalerie*t al.* 2012) is correlated with the crossing sea state. Although there are several studies related to the crossing sea states which discuss the interaction between wind-sea and swell, (Li *et al.* 2008) state that swell dissipation changes significantly after the crossing of two swell trains, and this is verified by space observations. The only remote sensing device that can measure the two-dimensional characteristics of ocean surface waves is the

synthetic aperture radar (SAR). In a recent study, the occurrence of crossing swells on a global ocean scale from space adds to a deeper understanding of the nature of oceans (Li 2016). Four distinct crossing swell pools were identified, their formation interpreted, and the propagation routes of ocean swells in the world's oceans depicted using the global wave data set of the spaceborne advanced SAR onboard the European Space Agency's satellite Envisat and the global wind data set of WindSat.

(Semedo*et al.* 2011), investigated the spatial pattern of the swell dominance of the earth's oceans, in terms of the wave field energy balance and wave field characteristics. They demonstrated that there are discernible variations in the major forms of variability of wind-sea and swell, especially in the Pacific and Atlantic Oceans. They provided a thorough climatology of the wave heights and directions for the wind-sea and swell components for the DJF (December, January, February) and JJA (June, July, August). Even along the extratropical storm zones, where the relative weight of the wind-sea section of the wave spectrum is largest, they discovered that the swell dominates the global wave field. Swell dominance is nearly always around 100% in low latitudes. The whole wave energy field is dominated by the swell energy.

(Ardhuin*et al.* 2009) studied swell dissipation across oceans for a number of storms using satellite data. Ocean swells were measured throughout ocean basins in a systematic manner between 2003 and 2007 using high quality data from a space-borne synthetic aperture radar. There were 22 estimates of the swell energy budget at peak periods of 13 to 18 seconds, thanks to ten storms that produced sufficient data. When small-amplitude swells dissipate across decay scales greater than 20,000 km, they can no longer be distinguished from viscous dissipation. Quite the reverse, though, since steep swells lose up to 65% of their energy over a span of just 2800 km. The researchers deduced that the observations and analysis pave the way for improved comprehension of air-sea fluxes during low wind circumstances, as well as more precise sea state predictions and hindcasts. (Sabique*et al.* 2012) studied the swell propagation from the Southern Indian Ocean and its contribution to the local wave climate in the Northern Indian Ocean using the ocean wave model, MIKE 21 SW. The model simulates wave heights from September 2008 to August 2009 for the Indian Ocean region (30°E–120°E and 60°S–30°N). They came to the conclusion that, in the Bay of Bengal, but not so much in the Arabian Sea, the swell dominance on the local wave environment decreases due to the effect of the southwest summer monsoon winds.

In the Northern Indian Ocean, the swell is a major factor otherwise for the other months of the year having important role in shaping the wave climate. In another study by (Glejin*et al.* 2016) the characteristics of long-period swells are described in the near shore regions of the eastern Arabian Sea. Measured data for 2 years and 3 locations shows long period waves having peak wave period greater than 18 seconds and low-amplitude waves having significant wave height less than a meter. For the year 2005, (Remya*et al.* 2016) studied how the North Indian Ocean high swell events are impacted by the meteorological conditions over the Southern Indian Ocean. They used both model data and in situ observations to analyze 10 high swell events for the given period. Their research demonstrates that the swells moving south of 30°S are what are responsible for these occurrences. In every instance, they saw a strong low-pressure system in the Southern Ocean three to five days prior to the large surge episodes in NIO. They came to the conclusion that, with adequate monitoring of the SIO's meteorological conditions, natural dangers along the shores of the NIO might be predicted at least two days in advance. (Zheng*et al.* 2018) calculated an intra seasonal swell index for the Indian Ocean. They came to the conclusion that waves typically took four to six days to propagate from the southern Indian Ocean's western region to the waters around Sri Lanka and Christmas Island, whereas they took two to four days to propagate from the southern Indian Ocean's eastern region to those areas. In order to provide a useful reference for swell wave power generation and ocean wave forecasting, they suggested studying the characteristics of swell propagation in each month as a future research. In this paper the impact of swell wave heights during the passage of a cyclone is studied in the BOB region, considering the pre-monsoon and post-monsoon influences.

2. DATA AND METHODOLOGY

ERA5 hourly estimates were considered, a fifth generation ECMWF (European Centre for Medium-Range Weather Forecasts) atmospheric reanalysis data, at 50 km spatial resolution. Swell wave heights were downloaded from 2014 to 2018 for the Bay of Bengal (BOB) region extending from 78^0 E to 98^0 E and 5^0 N to 25^0 N. Empirical orthogonal function (EOF) analysis was performed on the spatio-temporal data to obtain the maximum variability of the total variance. The EOF technique decomposes the space-time data into spatial modes ranked by their temporal variances. The main objective of the paper was to study the swell impact during cyclonic events. Thus, two cyclones were analyzed in the BOB region, one each occurring in the pre-monsoon and post-monsoon seasons. TITLI was a very severe cyclonic storm over the Bay of Bengal (07-13 October 2018) which occurred in the post-monsoon season. FANI was an extremely severe cyclonic storm over the west-central Bay of Bengal (26 April-05 May 2019) which occurred in the pre-monsoon season. EOF analysis was applied first on all the months of the above period (2014-2018) and then particularly for the months of May and October to study the spatial patterns of the BOB swell wave height parameter. The swell

wave heights and the significant wave heights were analyzed for particular events. EOF analysis (Wilks 1995; Jolliffe 2002) can be considered as a computational tool for data compression and dimensionality reduction. The EOF approach divides space-time distributed data into spatial modes sorted by temporal variance. The distinct modes are determined by calculating the eigenvalues and eigenvectors of a spatially weighted anomaly covariance matrix. The approach reduces the spatial variability of the data to a few eigenmodes. As a consequence, a collection of spatial modes and their corresponding temporal amplitude functions emerge. The spatial modes give information on spatial patterns, while the temporal amplitude functions characterise the data's dynamics.

3. RESULTS AND DISCUSSIONS

EOF analysis was applied to the BOB hourly swell wave heights for all the months from 2014 to 2018. Figure 1 shows the first principal component of the above data. The temporal pattern is of annual periodicity with maximum values during the southwest monsoon months and a minimum during the northeast monsoon months. The corresponding first spatial eigenmode exhibited an 80.33% variance with maximum loading towards the head and central BOB region. This may be attributed to the northeastward propagation of Southern Ocean swells. Figure 2 shows the dominant spatial pattern of the swell wave heights in the BOB region, considering all the months together.

Further, the swell pattern in the BOB region was studied for May and October representing the pre-monsoon and post-monsoon months. EOF analysis was performed next on the swell data from 2014-2018 separately for May and October. For May the total variance of the dominant mode was 69.3 % and for October 65.6 %, although the intensity of the maximum loading was more in October and towards the head BOB region. Figures 3 and 4 show the temporal and spatial patterns of the swell wave heights during May. Although there is no specific pattern of the first principal component, the amplitudes have an increasing trend from 2014 to 2018.For October the temporal and spatial patterns are given in Figures 5 and 6. The spatial pattern during May showed higher swell heights in the eastern-central BOB region whereas during October higher swell heights prevailed in the entire head-central BOB region. The cyclone FANI, which was an extremely severe cyclonic storm, made landfall along the Odisha coast on May 03, 2019 with 3-minute sustained winds of 215 km per hour and 1-minute sustained winds of 250 km per hour was a rare cyclone of such intensity to form in the Bay of Bengal in the month of April and cross the main land. On analysis using ERA5 data, during FANI cyclone, the maximum combined wind-wave and swell wave height on 03-May-00hrs 2019, off Odisha coast was 6 meters. It can be observed from Figures 7, 8, and 9 for the above case, the contribution due to swells was negligible and the wind generated waves were dominant during May in the east coast of India. The TITLI cyclone which made landfall on October 11, caused extensive damage due to strong wind and flood caused by extremely heavy rainfall along the east coast. A similar analysis during TITLI cyclone on 11-October-00 hrs 2018, showed (Figures 10, 11, 12) the maximum combined wind-wave and swell wave height was 4.4 meters off Odisha coast. However, in this case, the contribution due to swells (2.5 to 3 meters) was significant along with the wind-wave component. Thus, we can say during the post-monsoon months the swells impact significantly the cyclonic wave heights along the east coast in the BOB region in comparison to the pre-monsoon months.

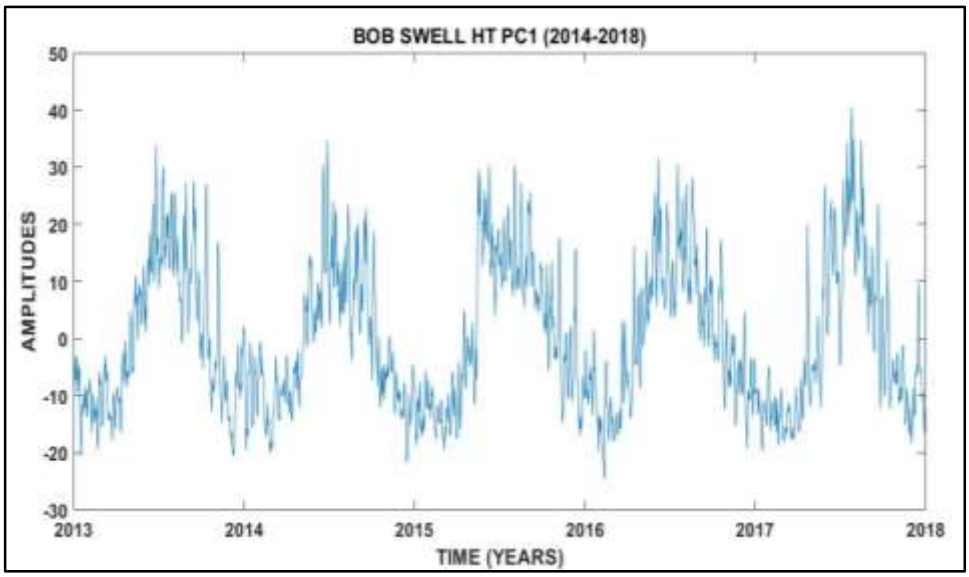

Figure 1. The first principal component of the BOB swell wave heights for 2014-2018.

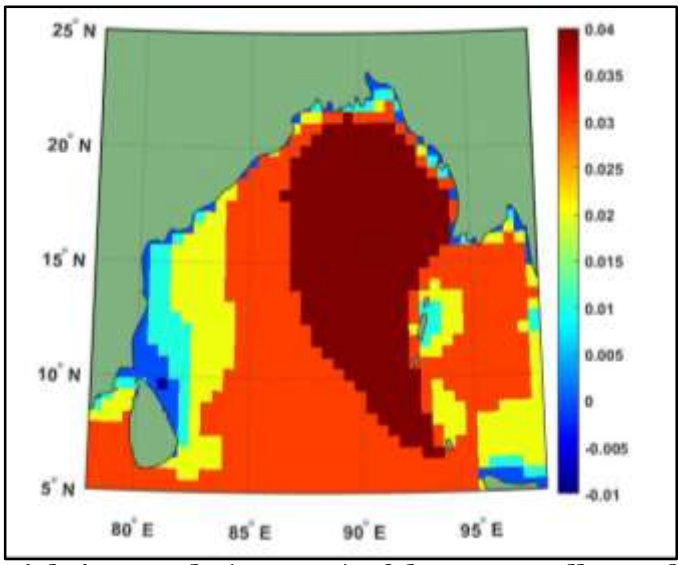

Figure 2. The first spatial eigenmode (80.33 %) of the BOB swell wave heights for the period 2014-2018.

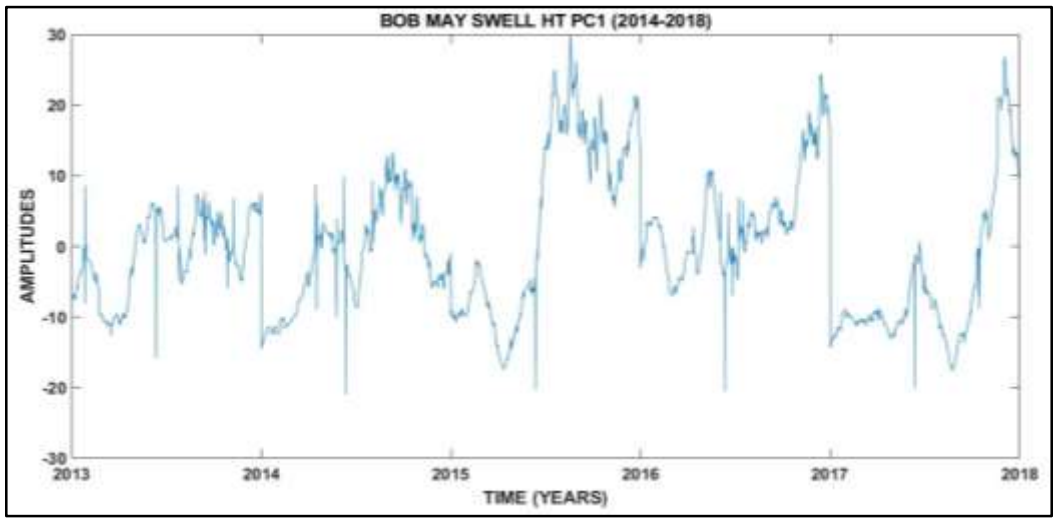

Figure 3. The first principal component of the BOB swell wave heights for May for the period 2014-2018.

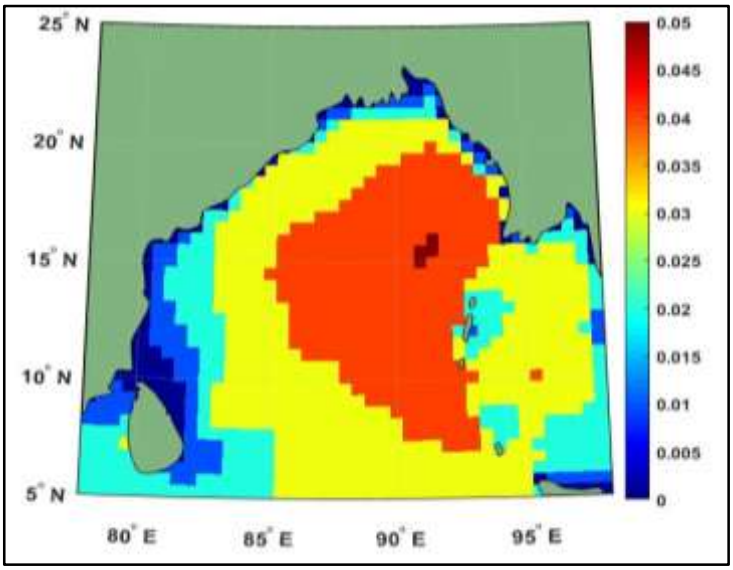

Figure 4. The first spatial eigenmode (69.3 %) of the BOB swell wave heights for May for the period 2014-2018.

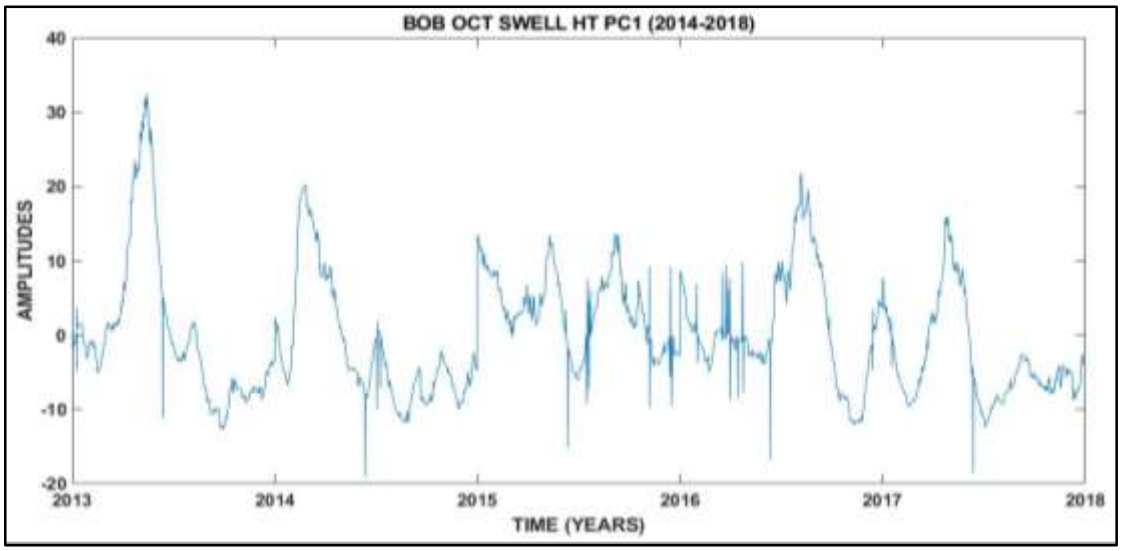

Figure 5. The first principal component of the BOB swell wave heights for October for the period 2014-2018.

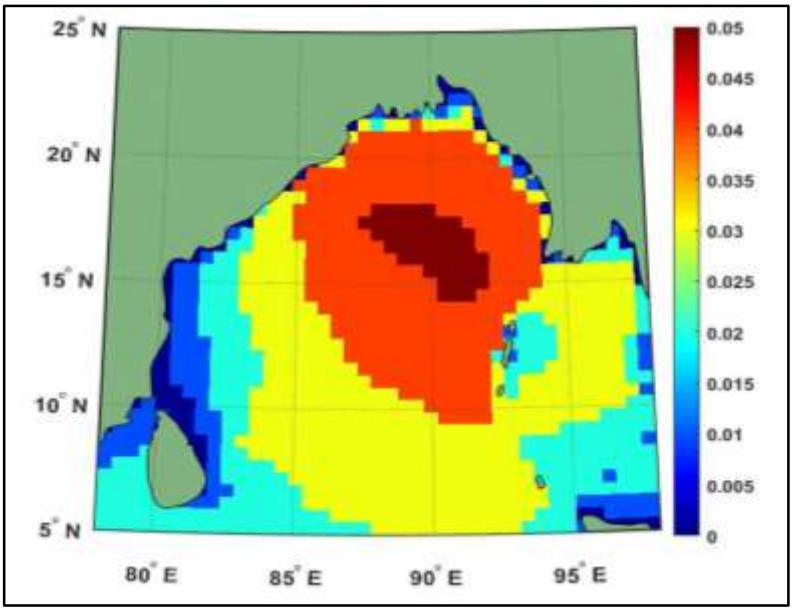

Figure 6. The first spatial eigenmode (65.6 %) of the BOB swell wave heights for October for the period 2014-2018.

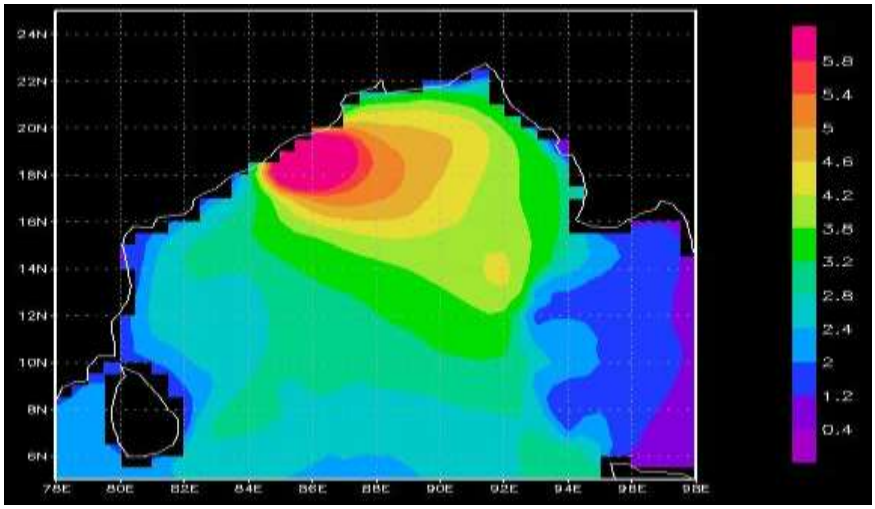

Figure 7. ERA5 combined wind-wave and swell wave height on 03-May-00hrs 2019 (FANI)

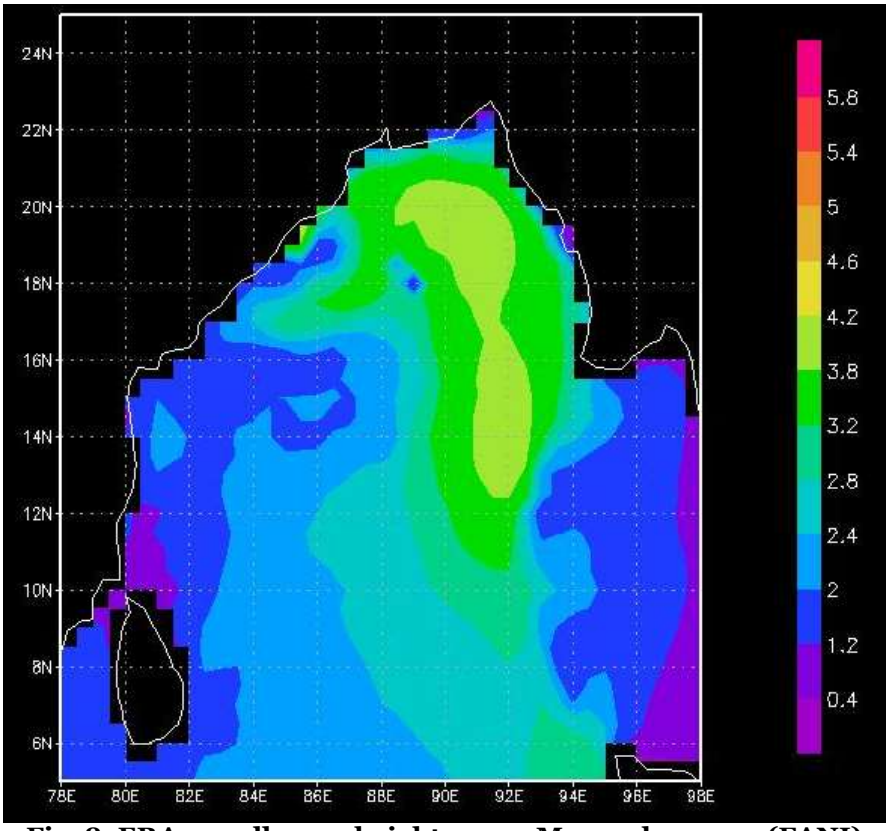

Fig. 8. ERA5 swell wave height on 03-May-00hrs 2019 (FANI)

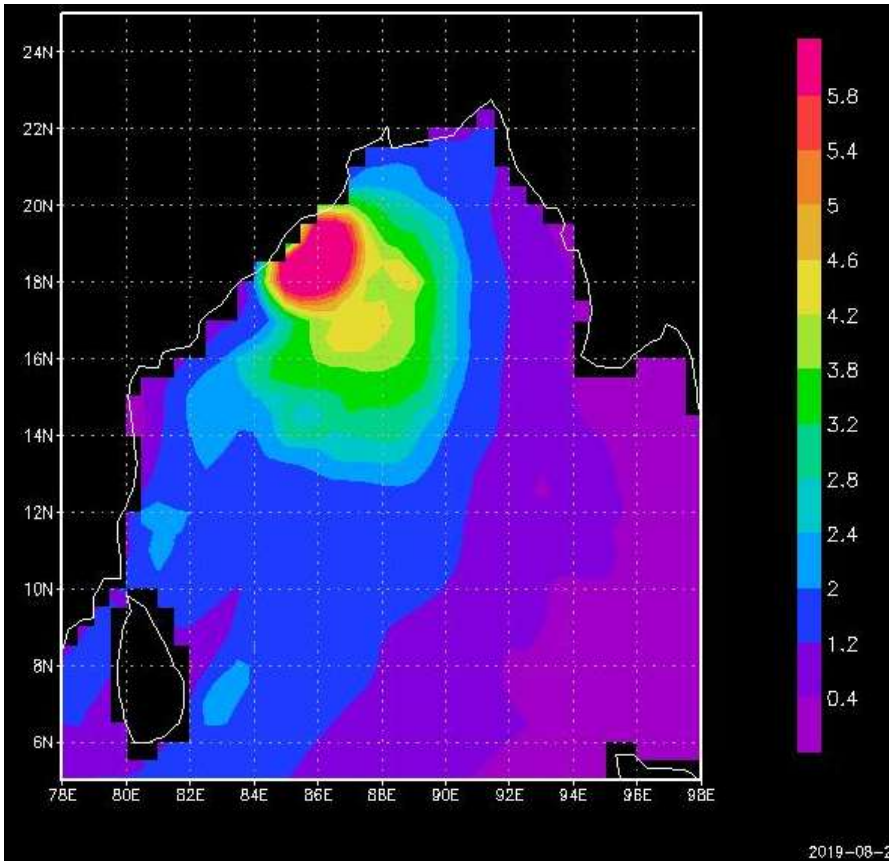

Fig. 9. ERA5 wind-wave height on 03-May-00hrs 2019 (FANI)

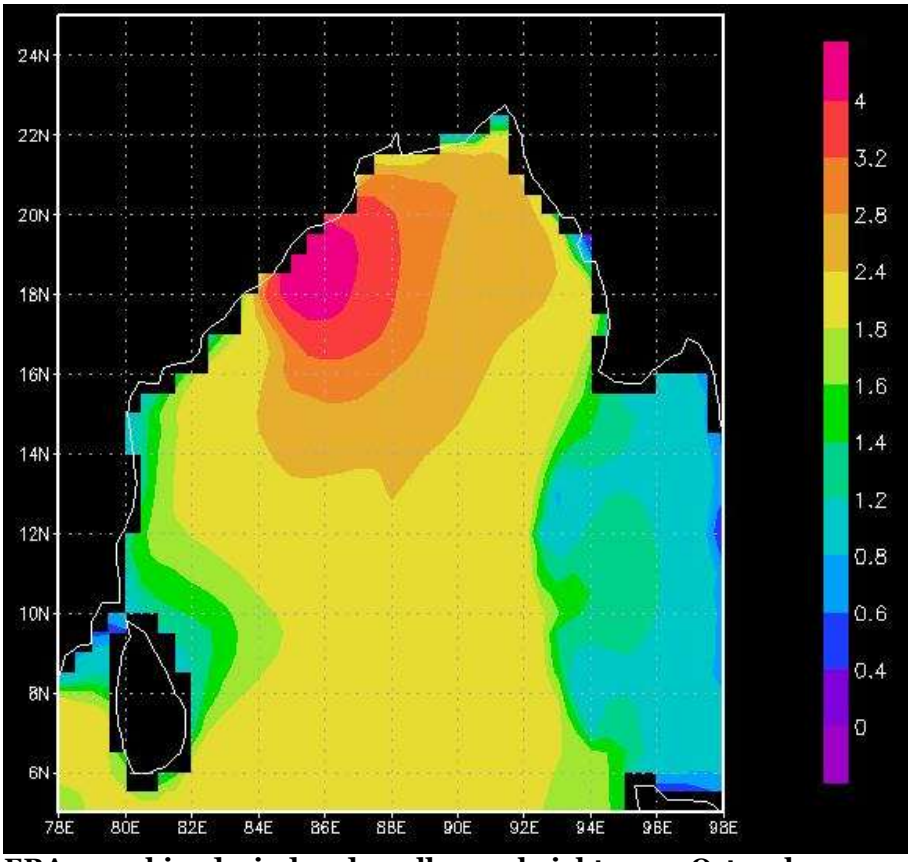

Fig. 10. ERA5 combined wind and swell wave height on 11-Oct-00hrs 2019 (TITLI)

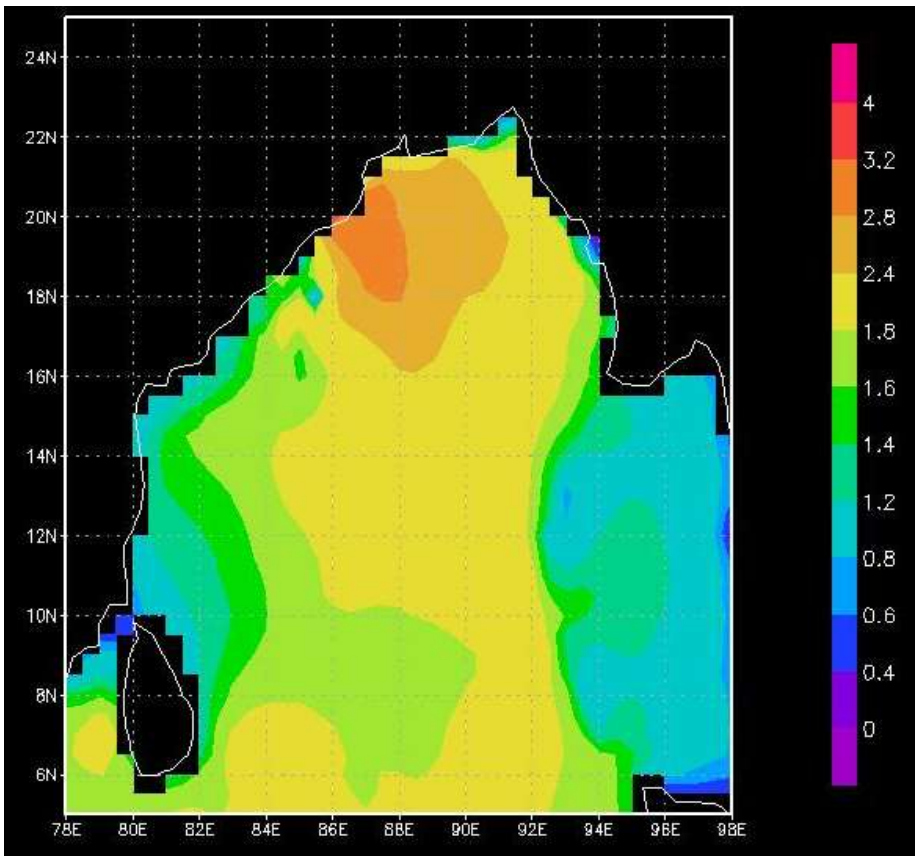

Fig. 11. ERA5 swell wave height on 11-Oct-00hrs 2019 (TITLI)

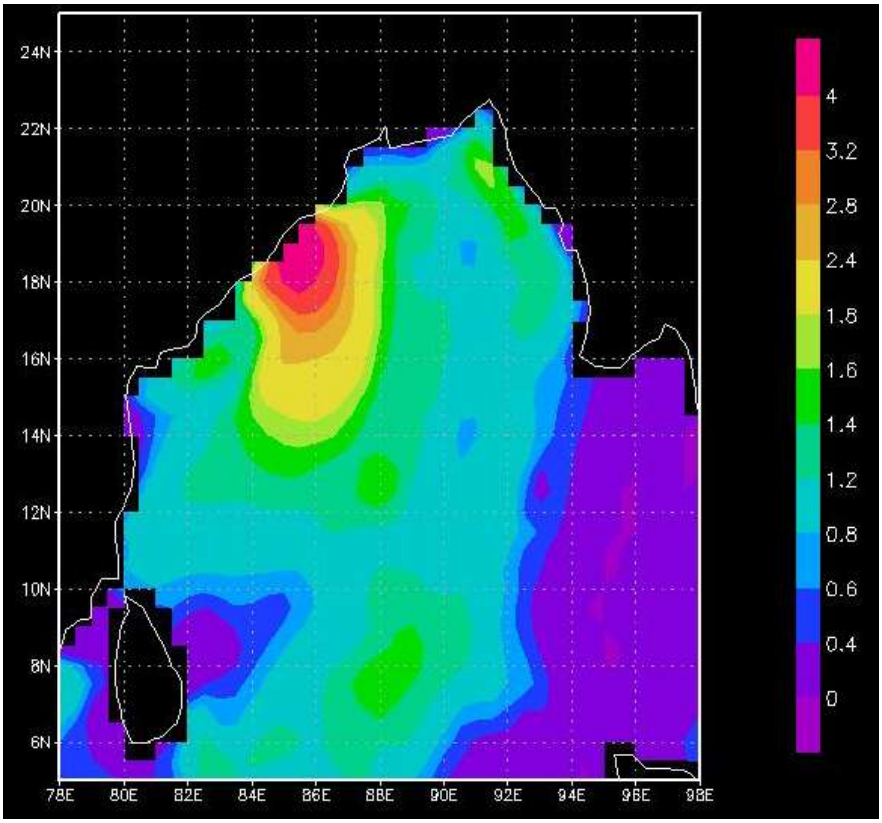

Fig. 12. ERA5 wind-wave height on 11-Oct-00hrs 2019 (TITLI)

4. CONCLUSIONS

Swell wave height data were considered and analyzed for the BOB region from 2014-2018. Applying EOF analysis to all the months together it was observed the temporal pattern was of annual periodicity corresponding to the monsoon oscillation. The spatial pattern showed maximum loading in the head and the central Bay region and the minimum loading along the south-east coast of India. EOF analysis applied only to swell data of May and October separately exhibited random pattern whereas the first spatial eigenmode in October covering a large area of the head and the central Bay had more intensity than May.EOF analysis revealed higher swell heights in October than May. The impacts of two cyclonic events occurring in the pre-monsoon and post-monsoon months were compared. The extremely severe cyclonic storm FANI made landfall on May 03, 2019 along the Odisha coast and the very severe cyclonic storm TITLI made landfall on October 11, 2019 along the east coast of India. A separate analysis of combined wind and swell wave heights, only swell wave heights and only wind wave heights on the above landfall days showed the swells contributed significantly in October only. For a particular location along the east coast, during FANI cyclone in May the combined wind-wave and swell wave height was about 6 meters. At this location the swell waves were insignificant whereas the wind-waves contributed remarkably. A similar analysis for the TITLI cyclone in October showed for a combined wind-wave and swell wave height of 4.4 meters, a swell wave of more than 3 meters could be observed. Thus in the post monsoon season along with prevailing higher swell waves in the BOB region, their impact on the cyclonic wave heights remains substantial.

Acknowledgements

The authors are thankful to ECMWF (European Centre for Medium-Range Weather Forecasts) for the ERA5 hourly data.

Research highlights

The temporal pattern of the swell wave heights in BOB shows annual periodicity corresponding to monsoon oscillation when all the months are considered together.
Monthly EOF analysis showed higher swell wave heights in October than May.
A separate analysis of combined wind and swell wave heights, only swell wave heights and only wind wave heights showed the swells contributed significantly to the cyclonic wave heights in October only.
In May the swell waves were insignificant whereas the wind-waves contributed remarkably during the passage of the cyclone.

References

1. Ardhuin F, Chapron B and Collard F2009 Observation of swell dissipation across oceans; *Geophys. Res. Lett.***36** L06607.https://doi.org/10.1029/2008GL037030
2. Bruns T, Lehner S, Li X M, Hessner K and Rosenthal W 2011 Analysis of an event of "Parametric Rolling" onboard RV "Polarstern" based on shipborne wave radar and satellite data; *IEEE J. Ocean. Eng*. **36(2)** 364-372.doi:10.1109/JOE.2011.2129630.
3. Cavaleri L, Bertotti L, Torrisi L, Bitner-Gregersen E, Serio M and Onorato M 2012 Rogue waves in crossing seas: The Louis Majesty accident; *J. Geophys. Res*. **117** C00J10.https://doi.org/10.1029/2012JC007923
4. Glejin J, Sanil V K, Amrutha M M, Singh J 2016 Characteristics of long-period swells measured in the near shore regions of eastern Arabian Sea;*International Journal of Naval Architecture and Ocean Engineering***8(4)** 312-319.http://drs.nio.org/drs/handle/2264/5008
5. Jolliffe I T 2002 Principal Component Analysis. Springer-Verlag, 2nd Edition, New York.
6. Li XM, Lehner S and He MX 2008 Ocean wave measurements based on satellite synthetic aperture radar (SAR) and numerical wave model (WAM) data - Extreme sea state and cross sea analysis; *International Journal of Remote Sensing***29(21)** 6403-6416.https://doi.org/10.1080/01431160802175546
7. Li X M 2016 A new insight from space into swell propagation and crossing in the global oceans; *Geophys.Res. Lett.***43**5202– 5209.https://doi.org/10.1002/2016GL068702
8. Sabique L, Annapurnaiah K, Balakrishnan T M and Srinivas N K 2012 Contribution of Southern Indian Ocean swells on the wave heights in the Northern Indian Ocean-A modeling study;*Ocean Engineering***43** 113-120.https://doi.org/10.1016/j.oceaneng.2011.12.024
9. Semedo A, Sušelj K, Rutgersson A and Sterl A 2011 A Global View on the Wind Sea and Swell Climate and Variability from ERA-40; *Journal of Climate***24** 1461-1479.https://doi.org/10.1175/2010JCLI3718.1
10. Remya P G, Vishnu S, Praveen B K, Balakrishnan Nair T M and Rohith B 2016 Teleconnection between the North Indian Ocean high swell events and meteorological conditions over the Southern Indian Ocean;*J. Geophys. Res. Oceans***121** 7476-7494.https://doi.org/10.1002/2016JC011723
11. Wilks D S 1995 Statistical Methods in the Atmospheric Sciences. Academic Press, San Diego.
12. Zhang Z and Li X M 2017 Global ship accidents and ocean swell-related sea states; *Nat. Hazards Earth Syst. Sci*. **17** 2041-2051.https://doi.org/10.5194/nhess-17-2041-2017
13. Zheng C W, Li C Y and Pan J 2018 Propagation route and speed of swell in the Indian Ocean;*J. Geophys. Res. Oceans* 123 8-21.https://doi.org/10.1002/2016JC012585